Neurosci. Bull. October, 2019, 35(5):815–825
https://doi.org/10.1007/s12264-019-00371-y

www.neurosci.cn
www.springer.com/12264

ORIGINAL ARTICLE

MicroRNA-365 Knockdown Prevents Ischemic Neuronal Injury by Activating Oxidation Resistance 1-Mediated Antioxidant Signals

Jia-Lin Mo[1,3] · Zhi-Guang Pan[2,3] · Xiao Chen[1,3] · Yu Lei[1,3] · Ling-Ling Lv[1,3] · Cheng Qian[1,3] · Feng-Yan Sun[1,2,3,4]

Received: 1 December 2018 / Accepted: 10 February 2019 / Published online: 11 April 2019

Abstract MicroRNA-365 (miR-365) is upregulated in the ischemic brain and is involved in oxidative damage in the diabetic rat. However, it is unclear whether miR-365 regulates oxidative stress (OS)-mediated neuronal damage after ischemia. Here, we used a transient middle cerebral artery occlusion model in rats and the hydrogen peroxide-induced OS model in primary cultured neurons to assess the roles of miR-365 in neuronal damage. We found that miR-365 exacerbated ischemic brain injury and OS-induced neuronal damage and was associated with a reduced expression of OXR1 (Oxidation Resistance 1). In contrast, miR-365 antagomir alleviated both the brain injury and OXR1 reduction. Luciferase assays indicated that miR-365 inhibited OXR1 expression by directly targeting the 3′-untranslated region of *Oxr1*. Furthermore, knockdown of OXR1 abolished the neuroprotective and antioxidant effects of the miR-365 antagomir. Our results suggest that miR-365 upregulation increases oxidative injury by inhibiting OXR1 expression, while its downregulation protects neurons from oxidative death by enhancing OXR1-mediated antioxidant signals.

Keywords MicroRNA · Ischemic stroke · Neuronal damage · Oxidative stress · Neuroprotection

Introduction

Tissue injury after cerebral ischemia is mediated by a variety of mechanisms, among which reactive oxygen species (ROS) play an important role [1]. The production of ROS in the brain after a stroke causes oxidative damage, further activating apoptosis, necrosis, and autophagy signaling pathways, leading to neuronal death [2, 3]. Timely enhancement of the antioxidant effects is considered to be a neuroprotective strategy for ischemic brain injury [4–6]. In general, antioxidant strategies include reducing ROS production and increasing ROS consumption. However, once a stroke occurs, reactive oxygen production in the brain increases rapidly, so reducing ROS accumulation would be neuroprotective against ischemic injury. Antioxidant enzymes, including superoxide dismutase, catalase (CAT), and glutathione peroxidase (GSH-Px), play crucial roles in detoxifying H_2O_2, a major type of ROS. Preclinical studies have demonstrated that increasing the amount of one of these detoxification enzymes can help prevent ischemia-induced OS in the brain [7–9].

OXR1, a member of a conserved family of proteins, has antioxidant properties [10, 11]. Deletion of *Oxr1* in *Saccharomyces cerevisiae* increases susceptibility to H_2O_2-induced injury [10], and knockdown of OXR1 reduces the integrity of mtDNA and increases OS-induced apoptosis in human cell lines [12]. Conversely, OXR1

Electronic supplementary material The online version of this article (https://doi.org/10.1007/s12264-019-00371-y) contains supplementary material, which is available to authorized users.

✉ Feng-Yan Sun
fysun@shmu.edu.cn

[1] Department of Neurobiology and Institute for Basic Research on Aging and Medicine, School of Basic Medical Sciences, Fudan University, Shanghai 200032, China

[2] Department of Neurosurgery, National Clinical Research Center for Aging and Medicine, Huashan Hospital, Shanghai Medical College, Fudan University, Shanghai 200032, China

[3] State Key Laboratory of Medical Neurobiology, School of Basic Medical Sciences, Fudan University, Shanghai 200032, China

[4] Shanghai Key Laboratory of Clinical Geriatric Medicine, Research Center on Aging and Medicine, Shanghai Medical College, Fudan University, Shanghai 200032, China

overexpression plays a protective role both in *in vitro* and *in vivo*. For example, forced expression of OXR1 protects cells against OS and aging in *Caenorhabditis elegans* [13] and prolongs the lifespan in *Drosophila melanogaster* [14]. Recently, OXR1 has been reported to reduce neurodegenerative pathogenesis and extend the survival of a mouse model of amyotrophic lateral sclerosis *via* its antioxidant effects [15–17]. Moreover, a previous study has reported that OXR1 has antioxidant effects by regulating the downstream antioxidant pathway, including the expression of the antioxidant enzymes CAT and GSH-Px [17, 18]. Therefore, we proposed that OXR1 may exert its neuroprotective effect on ischemic injury in the brain after stroke *via* its antioxidative actions.

MicroRNAs (miRs) are endogenous small ($\sim$ 22 nt) noncoding single-stranded RNAs that inhibit the expression of specific target messenger RNAs (mRNAs) by binding to their 3′-untranslated regions (UTRs)[19]. Increasing numbers of studies have shown that miRs play essential roles in neural disorders such as neurodegenerative diseases and ischemic stroke [20–24]. Recent studies have reported that miRs participate in pathophysiological processes after stroke, including excitotoxicity, OS, inflammation, blood-brain barrier damage, neuronal apoptosis, neurogenesis, and angiogenesis [2, 20, 23]. Our previous study demonstrated that miR-365 is upregulated in the brain following transient cerebral ischemia, and inhibits neurogenesis and repair [25]. Interestingly, the latest studies have reported that miR-365 increases retinal neuronal death by elevating OS in the diabetic rat [26, 27]. Notably, bioinformatics analysis showed that *Oxr1* is a potential target gene of miR-365. Therefore, we speculated that increased miR-365 in the brain after stroke might result in neuronal death probably *via* the inhibition of OXR1 expression, and down regulation of miR-365 might attenuate OS-mediated ischemic neuronal injury.

In this study, we determined the effects of miR-365 agomir and antagomir on neuronal damage in the adult rat transient middle cerebral artery occlusion (MCAO) model and in the primary neuron H_2O_2 model. Our main finding was that miR-365 increased ischemic neuronal damage through the elevation of OS by targeting *Oxr1*, and knockdown of miR-365 protected against ischemic neuronal injury *via* the activation of OXR1-mediated antioxidant signaling.

Materials and Methods

MiRNA and SiRNA Synthesis

The sequences of the oligonucleotides were as follows: miR-365-ago-sm (seed mutation) sense, 5′-UAAAGGCGCUAAAAAUCCUUAU-3′; antisense, 5′-AAGGAUUUUUAGCGCCUUUAUU-3′; *Oxr1* siRNA (siR-*Oxr1*) sense, 5′-GCGAAUAGUGGACGUUCUUTT-3′; antisense, 5′-AAGAACGUCCACUAUUCGCTT-3′; siRNA negative control (siR-nc) sense, 5′-UUCUCCGAACGUGUCACGUTT-3′; antisense, 5′-ACGUGACACGUUCGGAGAATT-3′. The sequences of miR-365 agomir (miR-365-ago), negative control (ago-nc), 106 miR-365 antagomir (miR-365-antag), and antagomir negative control (antag-nc) were demonstrated as previously described [25].

Animals

Male Sprague-Dawley rats (230 g–260 g) were obtained from the Shanghai Experimental Animal Center of the Chinese Academy of Sciences. All animal care protocols and experimental procedures were approved by the Institutional Animal Care Committee and Fudan University Shanghai Medical College Committee.

Transient MCAO and MiRNA Administration

As described previously [25], a 4-0 nylon monofilament (Sunbio Biotech, Beijing, China), was introduced into the internal carotid artery and left in place for 30 min. The rats in which cerebral blood flow dropped to 30%–40% during the procedure were used in subsequent tests. The mixture of miR oligomers (5 μL, 100 μmol/L) and Lipofectamine 2000 (5 μL) was incubated at room temperature and then injected into the contralateral lateral ventricle.

Neurological Score Measurement

Neurological deficits were assessed according to Longa's scale method [28]. The neurological score represents the severity of neurological deficits; higher scores represent more severe deficits.

Brain Section Preparation

As described previously [25], deeply anesthetized rats were perfused with 0.9% saline followed by 4% paraformaldehyde. The brain was removed and cryoprotected in a graded sucrose series. Coronal sections were cut at 30 μm and stored at − 20°C in a cryoprotectant solution.

Cresyl Violet Staining and Infarct Volume Measurement

Cresyl violet staining was used to identify viable cells. The areas of the infarct, contralateral hemisphere, and ipsilateral hemisphere were measured using an image-processing-analysis system (Q570IW, Leica, Wetzlar, Germany), and area multiplied by the distance between sections gave the

respective volumes. Infarct volume was calculated as the percentage of infarct volume relative to the volume of the contralateral hemisphere as described previously [29].

Immunohistochemical Staining and Cell Counting

Brain sections were incubated with anti-mouse-γH2AX (1:100; JBW301; Millipore, Billerica, MA, USA) overnight at 4°C, and then incubated with biotinylated secondary antibody and avidin-biotin-peroxidase complex (Vector Laboratories, Inc. Burlingame, CA). Immunoreactivity was detected with diaminobenzidine (DAB) (Sigma-Aldrich, Louis, MO, USA)[25] and γH2AX-positive cells were counted in five fields at the infarct border and are expressed as cells/mm^2.

Immunofluorescence Staining and Confocal Microscopy

For triple-labelling of NeuN, glial fibrillary acidic protein (GFAP), and γH2AX or OXR1, brain sections were incubated with primary antibodies at 4°C overnight followed by secondary antibodies for 1 h at 37°C. The following primary antibodies were used: anti-mouse γH2AX (1:100), anti-rabbit OXR1 (1:200; catalog 13514-1-AP; Proteintech, Chicago, IL, USA), anti-rabbit NeuN (1:200; ABN78; Millipore), or anti-mouse NeuN (1:200; catalog MAB377; Millipore), and anti-goat GFAP (1:200; catalog ab53554; Abcam, Cambridge, UK). Secondary antibodies were as follows: anti-mouse 488 (1:1,000; catalog A21202; Life Technologies, Carisbad, CA, USA), anti-rabbit 594 (1:1,000; catalog A21207; Life Technologies), and anti-goat647 (1:1,000; catalog A21447; Life Technologies). Immunoreactive signals were acquired with a confocal microscope (TCS SP8; Leica) as previously described [25].

Western Blotting Analysis

As described previously [25], 20 μg protein samples were subjected to SDS-PAGE and transferred onto PVDF membranes, which were blocked with 10% fat-free milk. Then, the membranes were incubated with anti-rabbit OXR1 (1:2,000) overnight at 4°C and anti-rabbit IgG-HRP (1:3,000; catalog sc-2004; Santa Cruz Biotechnology, CA, USA) for 1 h at room temperature. Bands were normalized to β-actin (1:10,000; catalog A5316; Sigma-Aldrich) and anti-mouse IgG-HRP (1:3,000; catalog sc-2005; Santa Cruz Biotechnology).

Luciferase Assay

Luciferase assays were performed as described previously [25]. Briefly, the 3′-UTR of *Oxr1*(1755 nt) contained in a reporter vector was cloned from cDNA from rat brain (forward primer: 5′-CCGCTCGAGATACAGTGCTCTTG GTTGTAGCAG-3′; reverse primer: 5′-TTTTCCTTTTGC GGCCGCCCTATGACCTTGTTGTAGCTGG-3′). PC12 cells were co-transfected with 200 ng reporter vector and 50 nmol/L miR oligomers. After 48 h, luciferase activity was assessed and expressed as the *Renilla*: firefly ratio.

qRT-PCRAnalysis

Extraction, reverse transcription, and amplification were performed as previously described [25]. The sequences of qRT-PCR primers for *Oxr1* were forward: 5′-CGCTTCGAGGACTACCTGAG-3′; reverse: 5′-TTTTGGCCAGTATCGGGTCC-3′. The actin, Rattus norvegicus-miR-365, and RNU6B primer sequences were as previously described [25].

Primary Cortical Neuron Culture and MiR Transfection

Primary neurons were isolated from 17- to 18-day Sprague-Dawley rat embryos as described previously [30]. The cells were seeded at 5×10^5 cells/ml in Neurobasal medium containing 2% B27 supplement under 5% CO_2 in a humidified incubator at 37°C. Cultures were transfected with 50 nmol/L agomir or antagomir or negative control (GenePharma, Shanghai, China)[31] using Lipofectamine 2000 (Invitrogen, Rockville, MD, USA). After 48 h, the cells were harvested for the detection of miRs and proteins.

Oxygen and Glucose Deprivation

Oxygen and glucose deprivation (OGD) was performed in primary neurons to simulate ischemia *in vivo*. As previously described [25], primary neurons were washed twice with deoxygenated Hanks' balanced salt solution and then incubated in deoxygenated glucose/serum-free Dulbecco's modified Eagle's medium. Then, the cultures were transferred to a hypoxic incubator chamber filled with 95% N_2/5% CO_2 at 37°C and left for 4 h. After OGD exposure, the cultures were maintained in complete medium under a normal atmosphere. MiR and protein analyses were performed at 12 h, 24 h, and 36 h of reoxygenation after OGD.

H_2O_2 Exposure

H_2O_2 was freshly prepared from 30% stock solution prior to each experiment, then added to the cultures and left for 24 h. To determine the role of miR-365 in the H_2O_2-induced neuronal death, we transfected miR-365-ago, ago-nc, miR-365-antag, or antag-nc (50 nmol/L) into primary neurons 24 h before H_2O_2 exposure. To assess the effects of OXR1 on the miR-365-

mediated neuronal death, we co-transfected miR-365-ago, ago-nc, miR-365-antag, or antag-nc (50 nmol/L) with *Oxr1* siRNA (50 nmol/L) into primary neurons 24 h before H_2O_2 exposure. Then, we harvested the cells after 24 h of H_2O_2 exposure for enzyme activity and cell viability analysis.

Catalase and Glutathione Peroxidase Activity Determination

The activity of CAT and GSH-Px in samples was determined using a Catalase Assay Kit (Beyotime, China) and Glutathione Peroxidase Assay Kit (Beyotime) based on the protocols provided by the manufacturer.

Cell Viability Assay

Cell viability was measured using Cell Counting Kit-8 (CCK-8; Dojindo Molecular Technologies, Ltd. Kumamoto, Japan) according to the manufacturer's instructions. The OD values were measured at 450 nm. Cell viability was calculated using the following formula: $(OD_{experiment} - OD_{blank})/(OD_{control} - OD_{blank}) \times 100\%$.

Statistical Analysis

Statistical analysis was performed with GraphPad Prism version 6.0 (GraphPad Software). Two-tailed Student's *t*-tests or one-way ANOVA with Tukey's *post-hoc* test were used to compare two groups or multiple groups, respectively. Results were considered statistically significant at $P < 0.05$.

Results

Treatment with MiR-365 Antagomir Reduces Brain Injury After MCAO

To investigate the role of miR-365 in ischemic brain injury, we injected ago-nc, miR-365-ago, antag-nc, or miR-365-antag into the contralateral ventricle of rats after MCAO. We confirmed that miR-365-ago increased, while miR-365-antag reduced the miR-365 levels in the ipsilateral striatum compared with ago-nc and antag-nc injection at 24 h after MCAO (Fig. 1A). Deficits in motor function were assessed by the neurological score at 24 h after MCAO. We found that miR-365-ago aggravated the motor deficits, where as miR-365-antag significantly improved motor function compared

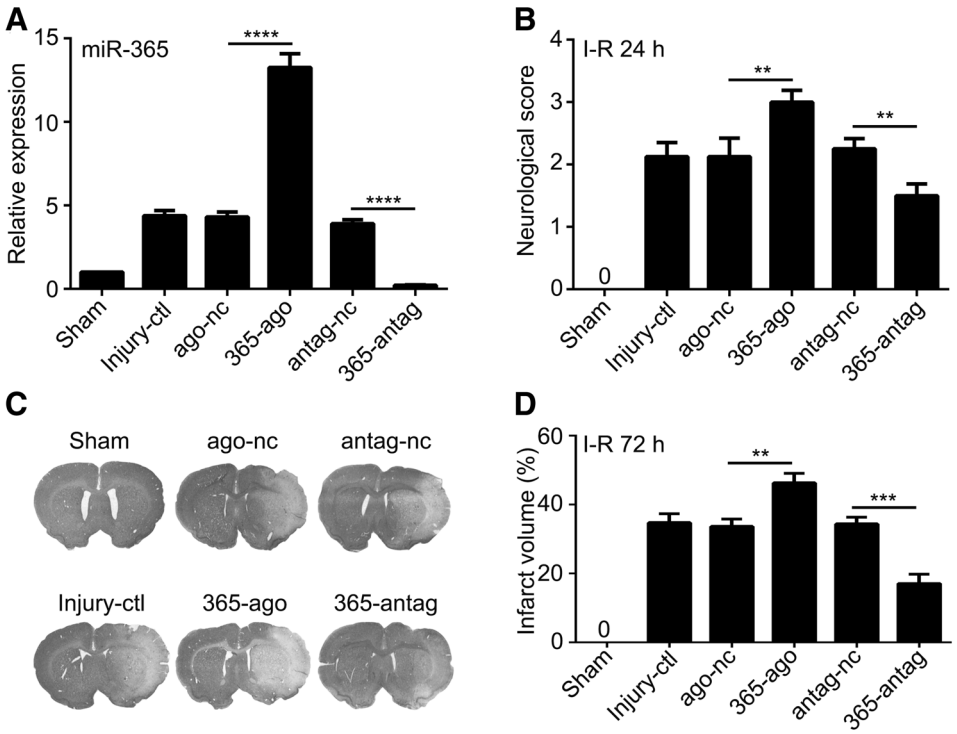

Fig. 1 MiR-365 antagomir reduces brain injury after ischemic stroke. **A** qRT-PCR analysis of miR-365 expression in the ischemic striatum 24 h after injection of miR-365 agomir (365-ago), agomir negative control (ago-nc), miR-365 antagomir (365-antag), or antagomir negative control (antag-nc) ($n = 3$). Injury control rats (Injury-ctl) were subjected to ischemia-reperfusion (I-R) without other interventions. **B** Neurological scores according to Longa's method 24 h after I-R ($n = 3$ in the sham group; $n = 8$ in the other groups). **C** Representative images of cresyl violet stained brain sections from rats 3 days after I-R (white indicates infarct area). **D** Infarct volume as a percentage of contralateral hemisphere volume ($n = 3$ in the sham group; $n = 6$ in the other groups). $^{**}P < 0.01$, $^{***}P < 0.001$, $^{****}P < 0.0001$, one-way ANOVA with Tukey's *post-hoc* test. Data are presented as the mean ± SEM.

with the corresponding negative control or injury-control group (Fig. 1B). Moreover, miR-365-ago significantly increased the infarct volume at 72 h after MCAO compared with the ago-nc or injury-control group. Conversely, miR-365-antag significantly reduced the infarct volume compared with the antag-nc or injury-control group (Fig. 1C, D). These results suggest that miR-365 exacerbates brain damage after ischemic stroke, while reduction of the miR-365 level in the ischemic brain provides neuroprotection.

MiR-365 Antagomir Reduces γH2AX Expression in Rat Brain After MCAO

Recent studies have shown that miR-365 increases neuronal death in the retina of diabetic rats by increasing OS [27]. OS causes the production of γH2AX, a marker of oxidative DNA damage [32–34]. Therefore, we studied the effects of miR-365 on γH2AX expression in the ischemic brain. After immunohistochemical staining, we counted γH2AX-positive ($\gamma H2AX^+$) cells in the brain 72 h after MCAO (Fig. 2A, B), and the results showed that ischemia increased the number of $\gamma H2AX^+$ cells in the ipsilateral striatum (Fig. 2C). MiR-365-ago further increased the number of $\gamma H2AX^+$ cells compared with ago-nc or injury-control. However, miR-365-antag significantly reduced the number of $\gamma H2AX^+$ cells compared with these controls (Fig. 2C). Furthermore, triple immunofluorescent labelling for NeuN, GFAP, and γH2AX showed that γH2AX was mainly expressed in neurons ($\gamma H2AX^+$/$NeuN^+$ cells) and not in astrocytes (Fig. 2D). These results suggested that miR-365 increases oxidative neuronal damage in the ischemic brain, and downregulation of miR-365 attenuates such damage.

OXR1 Expression is Reduced in Rat Brain and Primary Neurons After Ischemia

The next question was how miR-365 regulates oxidative damage in the brain after ischemic stroke. As noted above, OXR1 is a potential target of miR-365 based on bioinformatics prediction and its antioxidant effect plays a crucial role in neuroprotection [16, 17]. Here, we found that OXR1 protein first was significantly reduced and then gradually recovered in the ischemic brain and primary neurons under ischemia-like conditions (Fig. 3A, C). Interestingly, we found that the changes in expression of miR-365 *in vivo* and *in vitro* were opposite to those of OXR1 (Fig. 3B, D). In summary, these results suggested that ischemia induces

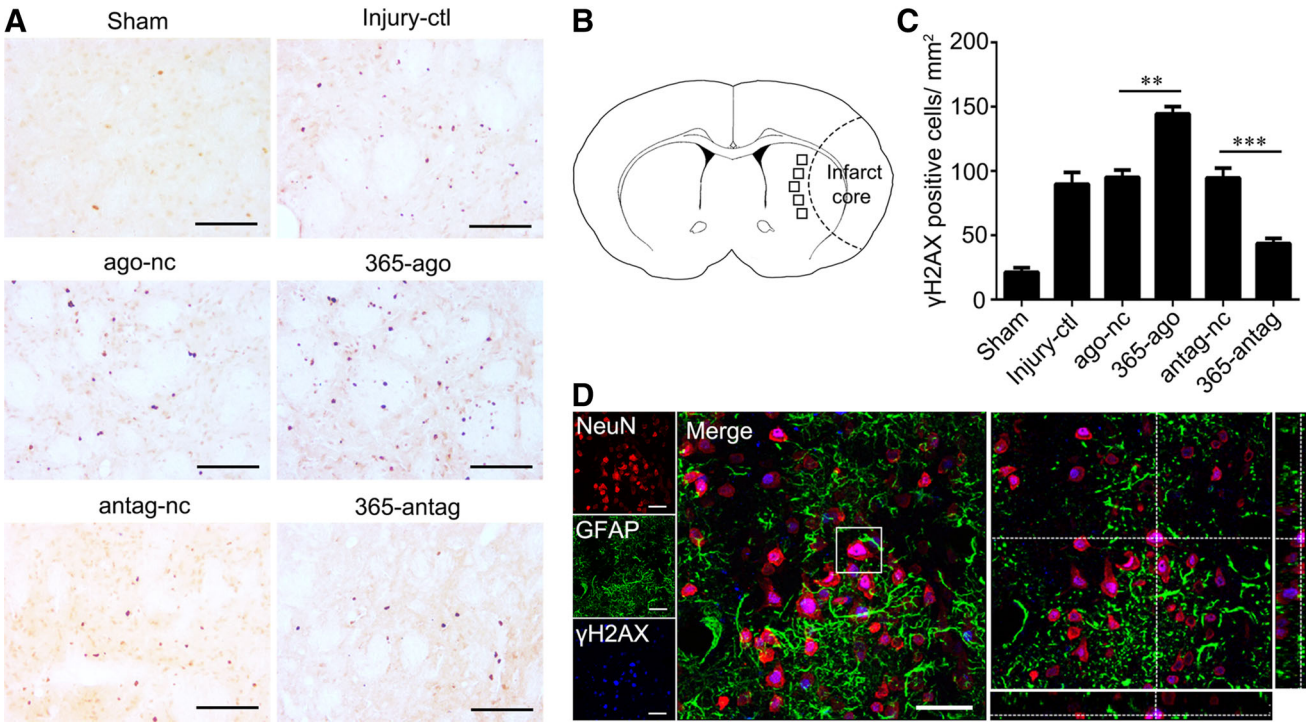

Fig. 2 MiR-365 antagomir reduces γH2AX expression in the ischemic striatum. **A** Representative images of immunolabeling of γH2AX in sections from rats 3 days after I-R (scale bars, 100 μm). **B** Schematic showing the areas in which immunoreactive cells were counted (five fields of view). **C** Numbers of γH2AX-positive cells (average of total positive cells/mm^2 in the five fields; $n = 3$ in the sham group; $n = 5$ in the other groups). **D** Representative images of immunofluorescent triple labeling of NeuN, γH2AX, and GFAP in sections from rats 3 days after MCAO (scale bars, 50 μm).$^{**}P < 0.01$, $^{***}P < 0.001$, one-way ANOVA with Tukey's *post-hoc* test. Data are presented as the mean ± SEM.

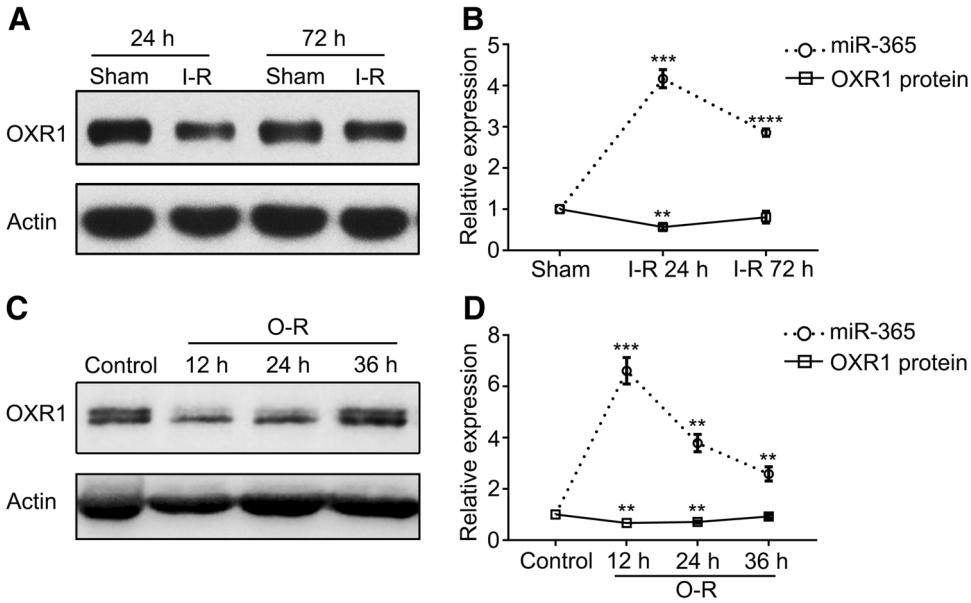

Fig. 3 OXR1 expression is reduced in the ischemia-induced striatum and primary neurons. **A**, **B** Expression levels of OXR1 protein and miR-365 in the ischemic striatum 24 and 72 h after I-R analyzed by Western blotting (WB) and qRT-PCR, respectively ($n = 3$ for qRT-PCR, $n = 4$ for WB). **C**, **D** Expression levels of OXR1 protein and miR-365 in primary neurons after 12, 24, and 36 h exposure to ischemia-like conditions analyzed by WB and qRT-PCR, respectively ($n = 3$). $^{**}P < 0.01$, $^{***}P < 0.001$, $^{****}P < 0.0001$ *versus* sham or control, unpaired two-tailed Student's *t*-test.

miR-365 upregulation and OXR1 downregulation *in vivo* and *in vitro*.

MiR-365 Antagomir Increases OXR1 Expression in Rat Brain After MCAO

We then assessed the effect of miR-365 on OXR1 expression in the brain after MCAO. The results showed that miR-365-ago reduced the levels of OXR1 protein at 24 h and 72 h after MCAO compared with the ago-nc or injury-control groups, while miR-365-antag markedly upregulated the OXR1 protein level at 24 h (Fig. 4A, B). Furthermore, triple fluorescent immunostaining for NeuN, GFAP, and OXR1 showed that OXR1 co-stained with NeuN ($OXR1^{+}/NeuN^{+}$) but not with GFAP, indicating that OXR1 is mainly expressed in neurons (Fig. 4C). These results suggested that miR-365 weakens the neuronal OXR1-mediated antioxidant capacity, and inhibition of miR-365 enhances the antioxidant effect.

MiR-365 Inhibits the Expression of OXR1 *Via* Targeting the 3′-UTR of *Oxr1*

Bioinformatics analysis revealed that the 3′-UTR of *Oxr1* contained two potential binding sites for miR-365(Fig. 5A). In order to determine whether miR-365 inhibits OXR1 expression by directly targeting the 3′-UTR of *Oxr1*, we performed dual luciferase gene reporter assays in PC12 cells. The full-length wild-type 3′-UTR of *Oxr1* was cloned and inserted into the pSiCheck vector to generate luciferase reporter plasmids. Moreover, we designed a mutant of miR-365 agomir (miR-365-ago-sm) with 3 base substitutions within the seed region (AAUGCCC to AAAGGCG) (Fig. 5B). After co-transfecting luciferase reporter plasmids with ago-nc, miR-365-ago, or miR-365-ago-sm in PC12 cells, we assessed the luciferase activity. The results showed that miR-365-ago significantly reduced the activity of luciferase reporter containing 3′-UTR of *Oxr1* compared with ago-nc. However, mutation of the seed regions completely abolished this effect of miR-365-ago (Fig. 5C). These results suggested that miR-365 directly targets the 3′-UTR of *Oxr1*.

Next, we analyzed the expression of OXR1 in rat primary neurons transfected with miR-365-ago, ago-nc, miR-365-antag, or antag-nc (Fig. 5D) and found that miR-365-ago reduced the OXR1 protein level compared with ago-nc. Conversely, miR-365-antag significantly increased the OXR1 protein compared with antag-nc. In addition, compared with the control group, neitherago-nc norantag-nc changed the expression of OXR1(Fig. 5E, F). Our results suggested that miR-365 directly modulates neuronal OXR1 expression by targeting the 3′-UTR of *Oxr1*.

Oxr1 siRNA Abolishes the Neuroprotective Effect of miR-365 Antagomir on Primary Neurons

Next, we induced oxidative damage in primary neurons with H_2O_2 to explore the role of the miR-365-OXR1 system in such damage. First, we confirmed that the appropriate concentration of H_2O_2 was 0.2 mmol/L (Fig. S1). OXR1 has been reported to regulate the expression of CAT and GSH-Px proteins, which detoxify

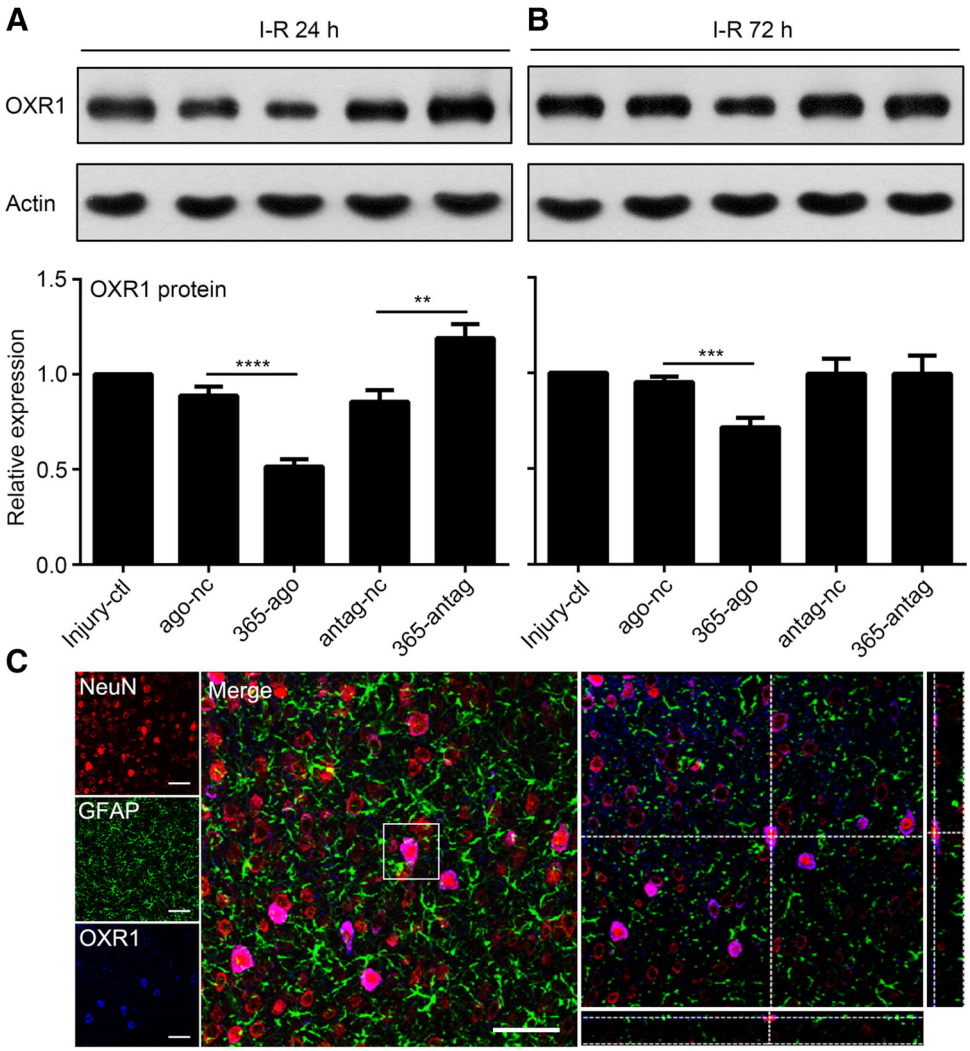

Fig. 4 MiR-365 antagomir increases OXR1 expression in the ischemic striatum. **A**, **B** Expression levels of OXR1 protein in the ischemic striatum 24 and 72 h after injection of 365-ago, ago-nc, 365-antag, or antag-nc analyzed by WB ($n = 4$ in the injury-control groups; $n = 5$ in the other groups). **C** Representative images of immunofluorescent triple labeling of NeuN, OXR1, and GFAP in brain sections from rats 3 days after MCAO (scale bars, 50 μm).$^{**}P < 0.01$, $^{***}P < 0.001$, $^{****}P < 0.0001$, one-way ANOVA with Tukey's *post-hoc* test. Data are presented as the mean ± SEM.

ROS [18, 35]. Therefore, we further analyzed the effects of the miR-365-OXR1 system on CAT and GSH-Px activity in the H_2O_2-induced oxidative damage model. We found that miR-365-ago significantly reduced the CAT and GSH-Px activity compared with the ago-nc and injury-control groups. Conversely, miR-365-antag significantly increased the CAT and GSH-Px activity compared with tag-nc and injury-control (Fig. 6A, C). However, *Oxr1* siRNA reduced the *Oxr1* mRNA to 30% of the control (Fig. S2) and inhibited CAT and GSH-Px activity. Moreover, knockdown of OXR1 expression by siRNA abolished the miR-365-antag-induced increase of CAT and GSH-Px activity (Fig. 6A–D). With this model we further found that, compared with the corresponding negative control or injury-control groups, miR-365-ago significantly reduced cell viability, while miR-365-antag improved it (Fig. 6E). More interestingly, OXR1-knockdown eliminated the protective effect of miR-365-antag against H_2O_2-induced oxidative neuronal damage (Fig. 6E, F). Taken together, these results suggested that the increase of miR-365 expression in the ischemic brain contributes to neuronal death by increasing oxidative damage through inhibiting the activation of OXR1-mediated CAT and GSH-Px.

Discussion

This study is the first to demonstrate that an increase in miR-365 after ischemic stroke leads to acute neuronal injury by targeting *Oxr1* in the rat. Moreover, miR-365-knockdown can effectively protect neurons from ischemic damage by increasing the activation of OXR1-mediated CAT and GSH-Px. These findings clearly revealed that reduction of endogenous miR-365 expression contributes to neuroprotection after stroke, which will help to develop therapeutic strategies to prevent neuronal death in the mammalian brain after trauma or ischemic injury.

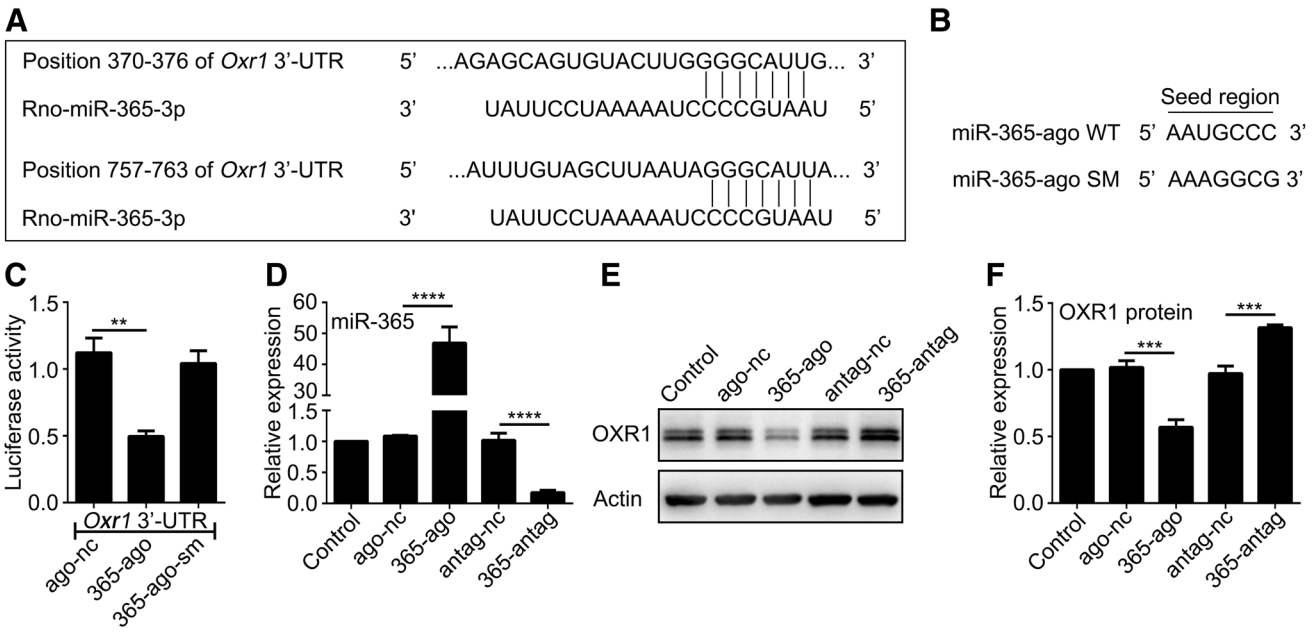

Fig. 5 MiR-365 directly targets OXR1 expression in primary neurons. **A** Nucleotide sequences of the predicted miR-365 binding sites in the 3′-UTR of *Oxr1*. Shown are the seed sequence (CCCGUAA) and wild-type miR-365 binding site (GGGCAUU). **B** The mutant seed sequence from mutant miR-365 agomir (miR-365-ago SM). Shown are the wild-type (CCCGUAA) and mutant (GCGGAAA) seed sequences. **C** Luciferase assays in PC12 cells 48 h after transfection of luciferase reporter plasmid containing the wild-type *Oxr1* 3′-UTR, together with ago-nc, 365-ago, or 365-ago-sm. Luciferase activity was calculated as the *Renilla*: firefly ratio ($n = 4$). **D** qRT-PCR analysis of miR-365 expression in primary neurons 48 h after transfection of 365-ago, ago-nc, 365-antag, or antag-nc ($n = 3$). **E**, **F** Expression levels of OXR1 protein in primary neurons 48 h after transfection of 365-ago, ago-nc, 365-antag, or antag-nc analyzed by Western blotting ($n = 4$). $^{**}P < 0.01$, unpaired two-tailed Student's *t*-test in C,$^{***}P < 0.001$, $^{****}P < 0.0001$, one-way ANOVA with Tukey's *post-hoc* test in D and F. Data are presented as the mean ± SEM.

Consistent with our previous report [25], miR-365 was markedly upregulated in the ischemic brain (Fig. 1A). Here, we found that upregulation of endogenous miR-365 in the ischemic brain accelerated neuronal damage, since inhibition of miR-365 expression by its antagomir significantly reduced neuronal oxidative DNA damage as indicated by $\gamma H2AX^+$ immunostaining (Fig. 2), infarct volume, and neurological deficit scores (Fig. 1B, D). In contrast, upregulation of miR-365 with ago mir aggravated the acute ischemic injury (Fig. 1). The results clearly showed that an increase of endogenous miR-365 expression in the ischemia-injured brain worsens the pathological process of acute neuronal death. It is well known that ischemic injury causes the adult brain to produce new neurons, thereby reconstructing distant [36] and local [37–39] neural networks. Neurogenesis is considered to be a fundamental process for brain repair after injury [40]. Combined with previous findings that miR-365 upregulation in the ischemia-injured brain inhibits repair by reducing neurogenesis from astroglial cells, whereas inhibiting miR-365 expression enhances the capacity of astroglial cells to transdifferentiate into new neurons [25], we have demonstrated that upregulation of endogenous miR-365 is detrimental to acute and chronic pathogenesis in the brain after ischemic injury and reduction of miR-365 is beneficial to neuroprotection and neural repair.

Therefore, we further analyzed the mechanism by which miR-365 modulates neuronal ischemic death. Our results showed that miR-365 participated in ischemia-induced oxidative DNA damage because administration of miR-365 agomir increased the number of $\gamma H2AX^+$ cells (Fig. 2) and reduced the activity of CAT and GSH-Px (Fig. 6). This finding is consistent with previous reports that miR-365 induces apoptosis in diabetic retinal neurons *via* reduction of antioxidant effects [26, 27]. As previously noted, OXR1 increases the expression of CAT and GSH-Px [18] and has antioxidant effects in *in vivo* and *in vitro* [12, 13, 15–17]. In this study, the changes of OXR1 protein expression and miR-365 expression were opposite in the ischemic brain and in primary neurons under ischemia-like conditions (Fig. 3), indicating that miR-365 targets OXR1 expression. We used bioinformatics analysis to identify two potential seed regions in the 3′-UTR of *Oxr1* for miR-365 binding (Fig. 5A). Therefore, we performed dual luciferase gene reporter assays to reveal that miR-365 can target the 3′-UTR seed regions of *Oxr1* and effectively inhibit the

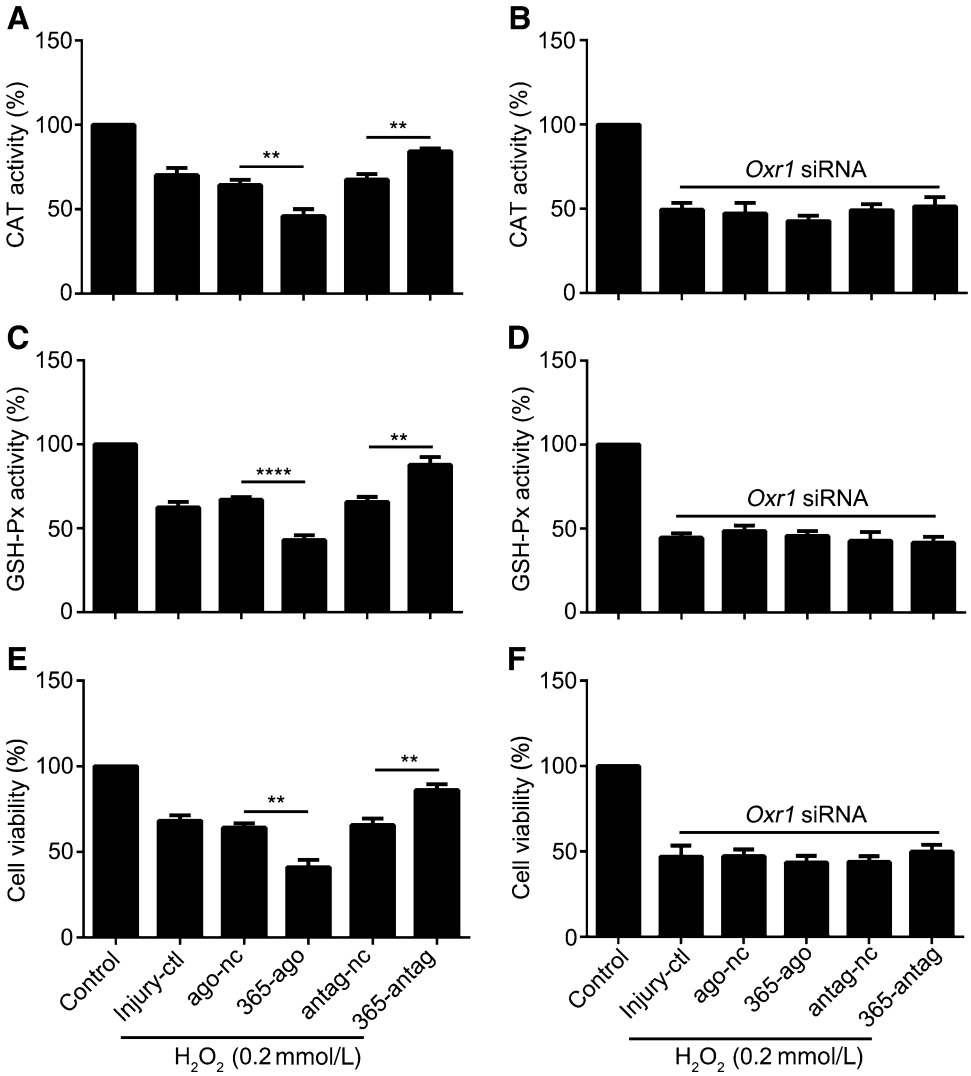

Fig. 6 *Oxr1* siRNA abolishes the protective effect of miR-365 antagomir on primary neurons. **A** CAT activity in primary neurons after transfection with 365-ago, ago-nc, 365-antag, or antag-nc and exposure to H_2O_2 ($n = 6$). **B** CAT activity in primary neurons after co-transfection of 365-ago, ago-nc, 365-antag, or antag-nc with *Oxr1* siRNA and exposure to H_2O_2 ($n = 6$). **C** GSH-Px activity in primary neurons after transfection with 365-ago, ago-nc, 365-antag, or antag-nc and exposure to H_2O_2 ($n = 6$). **D** GSH-Px activity in primary neurons after co-transfection of 365-ago, ago-nc, 365-antag, or antag-nc with *Oxr1* siRNA and exposure to H_2O_2 ($n = 6$). **E**, **F** Cell viability of primary neurons after co-transfection of 365-ago, ago-nc, 365-antag, or antag-nc with (**F**) or without (**E**) *Oxr1* siRNA and exposure to H_2O_2 ($n = 5$). $^{**}P < 0.01$, $^{****}P < 0.0001$, one-way ANOVA with Tukey's *post-hoc* test. Data are presented as the mean ± SEM.

expression of OXR1 protein in the ischemia-injured rat brain (Fig. 4A, B) and primary cultured neurons (Fig. 5E, F). We also demonstrated that this inhibitory effect of miR-365 was specific since miR-365 antagomir completely blocked this inhibition (Figs. 4 and 5). The next question was whether OXR1 production is involved in the miR-365-mediated antioxidant effects in injured neurons under ischemia-like conditions. Therefore, we knocked down OXR1 in primary cultured neurons with siRNA, and assessed the activity of CAT and GSH-Px and the survival of neurons under H_2O_2-induced OS. We interestingly found that OXR1 knockdown inhibited the activity of CAT and GSH-Px, further confirming that both of these enzymes are downstream of OXR1[18]. More importantly, *Oxr1* siRNA abolished the miR-365 antagomir-induced activation of CAT and GSH-Px as well as its neuroprotection in this model (Fig. 6), suggesting that endogenous miR-365 can cause oxidative damage and inhibit the activation of these two enzymes by inhibiting OXR1 production in neurons. This result is also consistent with previous reports in an amyotrophic lateral sclerosis model showing that reducing OXR1 is detrimental to neuronal survival and that OXR1 upregulation improves the pathological process and extends survival [13, 15–17]. Moreover, we noted that, after *Oxr1* siRNA treatment, miR-365 ago did not further increase the H_2O_2-induced oxidative neuronal death. This phenomenon may be due to the excessive regulation of OXR1 protein by siRNA in neurons, although the exact cause has yet to be explained. All together, we conclude that overproduction of miR-365 in the ischemic brain worsens oxidative neuronal injury by inhibiting OXR1-mediated CAT and GSH-Px antioxidant signals.

In summary, the present results demonstrate that endogenous miR-365 participates in the acute pathophysiological process of neuronal damage in the ischemic brain by modulating the OXR1-mediated CAT and GSH-Px antioxidant pathways. MiR-365 downregulation can inhibit ischemia-induced oxidative neuronal injury by enhancing

the OXR1-mediated antioxidant effects of CAT and GSH-Px and enhance acute neuroprotection. This study provides a new strategy for the development of novel the rapeutic targets for cerebral ischemic stroke.

Acknowledgements This work was supported by grants from the National Natural Science Foundation of China (81030020, 81571197, and 81771268) and the National Education Program of China (J0730860).

Conflict of interest The authors claim that there are no conflicts of interest.

References

1. Lipton P. Ischemic cell death in brain neurons. Physiol Rev 1999, 79: 1431–1568.
2. Zhao H, Han Z, Ji X, Luo Y. Epigenetic regulation of oxidative stress in ischemic stroke. Aging Dis 2016, 7: 295–306.
3. Li XJ, Zhang LM, Gu J, Zhang AZ, Sun FY. Melatonin decreases production of hydroxyl radical during cerebral ischemia-reperfusion. Acta Pharmacol Sin 1997, 18: 394–396.
4. Davis SM, Pennypacker KR. Targeting antioxidant enzyme expression as a therapeutic strategy for ischemic stroke. Neurochem Int 2017, 107: 23–32.
5. Ramos E, Patino P, Reiter RJ, Gil-Martin E, Marco-Contelles J, Parada E, *et al*. Ischemic brain injury: new insights on the protective role of melatonin. Free Radic Biol Med 2017, 104: 32–53.
6. Chamorro A, Dirnagl U, Urra X, Planas AM. Neuroprotection in acute stroke: targeting excitotoxicity, oxidative and nitrosative stress, and inflammation. Lancet Neurol 2016, 15: 869–881.
7. Baker K, Marcus CB, Huffman K, Kruk H, Malfroy B, Doctrow SR. Synthetic combined superoxide dismutase catalase mimetics are protective as a delayed treatment in a rat stroke model: a key role for reactive oxygen species in ischemic brain injury. J Pharmacol Exp Ther 1998, 284: 215–221.
8. Gu WP, Zhao H, Yenari MA, Sapolsky RM, Steinberg GK. Catalase over-expression protects striatal neurons from transient focal cerebral ischemia. Neuroreport 2004, 15: 413–416.
9. Ishibashi N, Prokopenko O, Weisbrot-Lefkowitza M, Reuhl KR, Mirochnitchenko O. Glutathione peroxidase inhibits cell death and glial activation following experimental stroke. Brain Res Mol Brain Res 2002, 109: 34–44.
10. Volkert MR, Elliott NA, Housman DE. Functional genomics reveals a family of eukaryotic oxidation protection genes. Proc Natl Acad Sci U S A 2000, 97: 14530–14535.
11. Durand M, Kolpak A, Farrell T, Elliott NA, Shao W, Brown M, *et al*. The OXR domain defines a conserved family of eukaryotic oxidation resistance proteins. BMC Cell Biol 2007, 8: 13.
12. Yang M, Luna L, Sorbo JG, Alseth I, Johansen RF, Backe PH, *et al*. Human OXR1 maintains mitochondrial DNA integrity and counteracts hydrogen peroxide-induced oxidative stress by regulating antioxidant pathways involving p21. Free Radic Biol Med 2014, 77: 41–48.
13. Sanada Y, Asai S, Ikemoto A, Moriwaki T, Nakamura N, Miyaji M, *et al*. Oxidation resistance 1 is essential for protection against oxidative stress and participates in the regulation of aging in *caenorhabditis elegans*. Free Radic Res 2014, 48: 919–928.
14. Kobayashi N, Takahashi M, Kihara S, Niimi T, Yamashita O, Yaginuma T. Cloning of cDNA encoding a bombyx mori homolog of human oxidation resistance 1 (OXR1) protein from diapause eggs, and analyses of its expression and function. J Insect Physiol 2014, 68: 58–68.
15. Finelli MJ, Liu KX, Wu Y, Oliver PL, Davies KE. Oxr1 improves pathogenic cellular features of ALS-associated FUS and TDP-43 mutations. Hum Mol Genet 2015, 24: 3529–3544.
16. Liu KX, Edwards B, Lee S, Finelli MJ, Davies B, Davies KE, *et al*. Neuron-specific antioxidant OXR1 extends survival of a mouse model of amyotrophic lateral sclerosis. Brain 2015, 138: 1167–1181.
17. Oliver PL, Finelli MJ, Edwards B, Bitoun E, Butts DL, Becker EB, *et al*. Oxr1 is essential for protection against oxidative stress-induced neurodegeneration. PLoS Genet 2011, 7: e1002338.
18. Jaramillo-Gutierrez G, Molina-Cruz A, Kumar S, Barillas-Mury C. The anopheles gambiae oxidation resistance 1 (OXR1) gene regulates expression of enzymes that detoxify reactive oxygen species. PLoS One 2010, 5: e11168.
19. Bartel DP. MicroRNAs: genomics, biogenesis, mechanism, and function. Cell 2004, 116: 281–297.
20. Zhou S, Ding F, Gu X. Non-coding RNAs as emerging regulators of neural injury responses and regeneration. Neurosci Bull 2016, 32: 253–264.
21. Li WY, Zhang WT, Cheng YX, Liu YC, Zhai FG, Sun P, *et al*. Inhibition of KLF7-targeting microRNA 146b promotes sciatic nerve regeneration. Neurosci Bull 2018, 34: 419–437.
22. Wang Y, Yang Z, Le W. Tiny but mighty: promising roles of microRNAs in the diagnosis and treatment of Parkinson's disease. Neurosci Bull 2017, 33: 543–551.
23. Li G, Morris-Blanco KC, Lopez MS, Yang T, Zhao H, Vemuganti R, *et al*. Impact of microRNAs on ischemic stroke: from pre- to post-disease. Prog Neurobiol 2018, 163–164: 59–78.
24. Fang X, Sun D, Wang Z, Yu Z, Liu W, Pu Y, *et al*. MiR-30a positively regulates the inflammatory response of microglia in experimental autoimmune encephalomyelitis. Neurosci Bull 2017, 33: 603–615.
25. Mo JL, Liu Q, Kou ZW, Wu KW, Yang P, Chen XH, *et al*. MicroRNA-365 modulates astrocyte conversion into neuron in adult rat brain after stroke by targeting Pax6. Glia 2018, 66:1263–1532.
26. Zheng K, Wang N, Shen Y, Zhang Z, Gu Q, Xu X, *et al*. Pro-apoptotic effects of microRNA-365 on retinal neurons by targeting IGF-1 in diabetic rats: an in vivo and in vitro study. J Diabetes Investig 2018, 9:1041–1051.
27. Wang J, Zhang J, Chen X, Yang Y, Wang F, Li W, *et al*. MiR-365 promotes diabetic retinopathy through inhibiting Timp3 and increasing oxidative stress. Exp Eye Res 2018, 168: 89–99.
28. Longa EZ, Weinstein PR, Carlson S, Cummins R. Reversible middle cerebral-artery occlusion without craniectomy in rats. Stroke 1989, 20: 84–91.
29. Swanson RA, Morton MT, Tsao-Wu G, Savalos RA, Davidson C, Sharp FR. A semiautomated method for measuring brain infarct volume. J Cereb Blood Flow Metab 1990, 10: 290–293.
30. Wu KW, Kou ZW, Mo JL, Deng XX, Sun FY. Neurovascular coupling protects neurons against hypoxic injury via inhibition of potassium currents by generation of nitric oxide in direct neuron and endothelium cocultures. Neuroscience 2016, 334: 275–282.
31. Ma Q, Zhao H, Tao Z, Wang R, Liu P, Han Z, *et al*. MicroRNA-181c exacerbates brain injury in acute ischemic stroke. Aging Dis 2016, 7: 705–714.
32. Redon CE, Dickey JS, Bonner WM, Sedelnikova OA. Gamma-H2AX as a biomarker of DNA damage induced by ionizing radiation in human peripheral blood lymphocytes and artificial skin. Adv Space Res 2009, 43: 1171–1178.
33. Downs JA, Lowndes NF, Jackson SP. A role for saccharomyces cerevisiae histone H2A in DNA repair. Nature 2000, 408: 1001–1004.

34. Kuo LJ, Yang LX. Gamma-H2AX - a novel biomarker for DNA double-strand breaks. In Vivo 2008, 22: 305–309.
35. He L, He T, Farrar S, Ji L, Liu T, Ma X. Antioxidants maintain cellular redox homeostasis by elimination of reactive oxygen species. Cell Physiol Biochem 2017, 44: 532–553.
36. Sun X, Zhang QW, Xu M, Guo JJ, Shen SW, Wang YQ, *et al*. New striatal neurons form projections to substantia nigra in adult rat brain after stroke. Neurobiol Dis 2012, 45: 601–609.
37. Hou SW, Wang YQ, Xu M, Shen DH, Wang JJ, Huang F, *et al*. Functional integration of newly generated neurons into striatum after cerebral ischemia in the adult rat brain. Stroke 2008, 39: 2837–2844.
38. Duan CL, Liu CW, Shen SW, Yu Z, Mo JL, Chen XH, *et al*. Striatal astrocytes transdifferentiate into functional mature neurons following ischemic brain injury. Glia 2015, 63: 1660–1670.
39. Darsalia V, Heldmann U, Lindvall O, Kokaia Z. Stroke-induced neurogenesis in aged brain. Stroke 2005, 36: 1790–1795.
40. Zhang QW, Deng XX, Sun X, Xu JX, Sun FY. Exercise promotes axon regeneration of newborn striatonigral and corticonigral projection neurons in rats after ischemic stroke. PLoS One 2013, 8: e80139.